The Plant Cell, Vol. 30: 1062–1076, May 2018, www.plantcell.org © 2018 ASPB.

Check for updates

# The Ubiquitin E3 Ligase PRU1 Regulates WRKY6 Degradation to Modulate Phosphate Homeostasis in Response to Low-Pi Stress in Arabidopsis

**Qing Ye, Hui Wang, Tong Su, Wei-Hua Wu, and Yi-Fang Chen[1]**

State Key Laboratory of Plant Physiology and Biochemistry, College of Biological Sciences, China Agricultural University, Beijing 100193, China

ORCID IDs: 0000-0002-0642-5523 (W.-H.W.); 0000-0002-8603-3668 (Y.-F.C.)

**Since phosphorus is an essential nutrient for plants, plants have evolved a number of adaptive mechanisms to respond to changes in phosphate (Pi) supply. Previously, we reported that the transcription factor WRKY6 modulates Pi homeostasis by downregulating *PHOSPHATE1* (*PHO1*) expression and that WRKY6 is degraded during Pi starvation in *Arabidopsis thaliana*. However, the molecular mechanism underlying low-Pi-induced WRKY6 degradation was unknown. Here, we report that a ubiquitin E3 ligase, PHOSPHATE RESPONSE UBIQUITIN E3 LIGASE1 (PRU1), modulates WRKY6 protein levels in response to low-Pi stress. A *pru1* mutant was more sensitive than the wild type to Pi-deficient conditions, exhibiting a reduced Pi contents in the shoot, similar to the *pho1-2* mutant and *WRKY6*-overexpressing line. PRU1 interacted with WRKY6 in vitro and in vivo. Under low-Pi stress, the ubiquitination and subsequent degradation of WRKY6, as well as the consequential enhancement of *PHO1* expression, were impaired in *pru1*. PRU1 complementation lines displayed no obvious differences compared with wild-type plants. Further genetic analysis showed that disruption of *WRKY6* abolished the low-Pi sensitivity of *pru1*, indicating that WRKY6 functioned downstream of PRU1. Taken together, this study uncovers a mechanism by which PRU1 modulates Pi homeostasis, through regulating the abundance of WRKY6 in response to low-Pi stress in Arabidopsis.**

## INTRODUCTION

Phosphorus (P) is a major essential nutrient for plant growth and development (Raghothama, 1999), and phosphate (Pi, $H_2PO_4^-$) is the main form of phosphorus that is absorbed by plants (Chiou and Lin, 2011; López-Arredondo et al., 2014). The Pi concentration in soil is typically 10 μM or less (Raghothama, 1999), which results in Pi starvation and impacts plant growth and survival. Pi uptake by plants occurs mainly through Pi transporters. The *Arabidopsis thaliana* genome contains at least nine members of the PHOSPHATE TRANSPORTER1 (PHT1) family (Okumura et al., 1998; Mudge et al., 2002), with PHT1;1 and PHT1;4 playing a major role in acquiring Pi from the soil (Shin et al., 2004).

Arabidopsis PHOSPHATE1 (PHO1) participates in Pi transfer from roots to shoots (Poirier et al., 1991; Hamburger et al., 2002), and the *pho1* mutant only accumulates 24 to 44% as much Pi in the shoots as wild-type plants (Poirier et al., 1991). PHO1 is located in root stelar cells (Hamburger et al., 2002), which is consistent with its function in Pi efflux out of cells and into xylem. PHO1-mediated Pi export is associated with its localization to the Golgi and *trans*-Golgi networks (Arpat et al., 2012). Under Pi-deficient conditions, *PHO1* expression increases significantly (Stefanovic et al., 2007; Ribot et al., 2008; Chen et al., 2009). The Arabidopsis transcription factors WRKY6 and WRKY42 negatively regulate *PHO1* expression under Pi-sufficient conditions. Furthermore, during Pi starvation WRKY6 and WRKY42 are degraded via 26S proteosome-mediated proteolysis (Chen et al., 2009; Su et al., 2015), suggesting that a ubiquitin-proteasome system is involved in maintaining Pi homeostasis.

Ubiquitination of proteins is a multistep reaction, requiring three enzymes: E1, ubiquitin-activating enzyme; E2, ubiquitin-conjugating enzyme; and E3, ubiquitin ligase (Sadanandom et al., 2012). The Arabidopsis genome encodes two E1s, at least 37 E2s, and over 1300 potential E3s (Smalle and Vierstra, 2004). However, the role of the ubiquitin-proteasome system in the plant's response to low-Pi stress is unclear. Arabidopsis *SIZ1* encodes a small ubiquitin-like modifier E3 ligase, and its T-DNA insertion mutant, *siz1*, displays an exaggerated Pi starvation response (Miura et al., 2005). SIZ1 sumoylates the transcription factor PHR1 (Miura et al., 2005); however, the consequence of PHR1 sumoylation is unknown. An Arabidopsis RING-type ubiquitin E3 ligase, NITROGEN LIMITATION ADAPTATION (NLA), plays a role in maintaining nitrate-dependent Pi homeostasis (Kant et al., 2011). Recently, NLA was found to modulate the degradation of PHT1s under Pi-sufficient conditions (Lin et al., 2013; Park et al., 2014), and the *nla* mutant was shown to accumulate high levels of Pi due to an increase in the abundance of PHT1s (Lin et al., 2013). Arabidopsis PHO2, a ubiquitin-conjugating enzyme, mediates the degradation of PHT1s and PHO1 (Liu et al., 2012; Huang et al., 2013), and its mutant *pho2* displays Pi toxicity due to enhanced Pi uptake and root-to-shoot transfer (Aung et al., 2006; Bari et al., 2006).

In this study, we found that a *pru1* (*phosphate response ubiquitin E3 ligase1*) mutant displayed a similar phenotype to the

[1] Address correspondence to chenyifang@cau.edu.cn.
The author responsible for distribution of materials integral to the findings presented in this article in accordance with the policy described in the Instructions for Authors (www.plantcell.org) is: Yi-Fang Chen (chenyifang@cau.edu.cn).
www.plantcell.org/cgi/doi/10.1105/tpc.17.00845

## IN A NUTSHELL

**Background:** Phosphorus is a major essential nutrient for plant growth and development, and phosphate (Pi) is the main form of phosphorus that is absorbed by plants and translocated from roots to shoots. Arabidopsis PHOSPHATE1 (PHO1) protein participates in Pi transfer from roots to shoots, and the expression of the PHO1 gene is down-regulated by the transcription factor WRKY6 under Pi-sufficient conditions. The WRKY6 protein is degraded during Pi starvation, and then the repression of PHO1 by WRKY6 is released.

**Question:** WRKY6 is degraded under low-Pi stress, and then PHO1 gene expression is elevated. How are these processes integrated? Is there a key regulator in modulating the degradation of WRKY6?

**Findings:** We found that Arabidopsis PRU1 modulates Pi transfer from roots to shoots in response to low-Pi stress. PRU1 functions as an ubiquitin E3 ligase. Under Pi-sufficient conditions, WRKY6 represses PHO1 expression; under Pi-deficient conditions, PRU1 ubiquitinates WRKY6, which targets the protein for proteasome-dependent degradation, and then the PHO1 expression is enhanced. Thus PRU1 modulates Pi homeostasis by regulating the abundance of WRKY6 in response to low-Pi stress.

**Next steps:** Pi homeostasis is precisely modulated to adapt to environmental changes in Pi availability. Further investigation into the regulation of Pi translocation is needed. In addition, it is unclear how PRU1 activity is modulated in response to low-Pi stress.

*pho1-2* mutant and *WRKY6*-overexpressing line, including increased sensitivity to low-Pi and reduced shoot Pi contents. Low-Pi-induced WRKY6 degradation and *PHO1* accumulation were also impaired in the *pru1* mutant. Further biochemical and genetic data revealed that PRU1 modulates WRKY6 degradation under low-Pi stress. This work uncovers a crucial regulatory pathway in the response to low-Pi stress in Arabidopsis.

## RESULTS

### The *pru1* Mutant Is Defective in Pi Transfer from Roots to Shoots under Low-Pi Stress

We previously reported that under Pi-sufficient conditions, the transcription factor WRKY6 modulates Pi transfer by negatively regulating *PHO1* expression and that during Pi starvation, WRKY6 is degraded by a ubiquitin-proteasome pathway, releasing the WRKY6-mediated repression of *PHO1* (Chen et al., 2009). Therefore, we initiated an investigation to identify the ubiquitin E3 ligase responsible for modulating the degradation of WRKY6. We did not identify an E3 ligase that can interact with WRKY6 using a yeast two-hybrid screen. We thus obtained 459 Arabidopsis lines with T-DNA insertions in putative E3 ligases from the ABRC stock center and verified 425 of these lines as homozygous *e3* mutants (Supplemental Data Set 1). Plants accumulate anthocyanin in aerial potions in response to low-Pi stress, which results in brown-colored leaves (Marschner, 2012). Our previous study showed that the *pho1-2* mutant and *WRKY6*-overexpressing line (*35S:WRKY6-9*) were sensitive to low-Pi stress, with more accumulation of anthocyanin in young leaves than in wild-type plants (Chen et al., 2009). We next assessed the phenotypes of the homozygous *e3* mutants under Pi-deficient conditions and selected the low-Pi-sensitive *e3* mutants. The low-Pi-sensitive phenotypes of *e3* mutants were confirmed with seeds from two independent harvests. We identified a T-DNA insertion line (Salk_069673C), which we named *pru1*, that exhibited increased sensitivity to low-Pi stress, similar to *35S:WRKY6-9*. We designated the affected gene *PRU1*. PRU1 is an F-box/RNI-like/FBD-like domain-containing protein (TAIR, http://www.arabidopsis.org/servlets/TairObject?&id=37473type=locus). Although there are at least 41 F-box/RNI-like/FBD-like domain-containing proteins in the Arabidopsis genome, PRU1 did not have a homolog in Arabidopsis (Supplemental Figure 1A). We conducted a BLASTp analysis in NCBI (www.ncbi.nlm.nih.gov) using the PRU1 protein and identified several PRU1 orthologs in grape (*Vitis vinifera*), maize (*Zea mays*), *Medicago truncatula*, and soybean (*Glycine max*), but not in rice (*Oryza sativa*) (Supplemental Figure 1B).

To confirm that the low-Pi sensitivity of the *pru1* mutant was due to the T-DNA insertion in *PRU1*, we generated complementation lines. *PRU1* transcript was almost absent in the *pru1* mutant, and the complementation lines (COM5 and COM7) displayed similar levels of *PRU1* transcript as wild-type plants (Figure 1A). Our previous study showed that the *pho1-2* mutant and *WRKY6*-overexpressing lines were sensitive to low-Pi conditions (Chen et al., 2009). In Arabidopsis, PHO1 mediates Pi translocation from roots to shoots, and the *pho1* mutants show reduced shoot growth and accumulate anthocyanin when grown in soil (Supplemental Figure 2A; Poirier et al., 1991; Hamburger et al., 2002; Liu et al., 2012). Although *PHO1* transcript abundance was similar between *pho1-2* and wild-type plants (Supplemental Figure 2B), the *pho1-2* mutant contained a point mutation, C1018T, in *PHO1*, which caused a premature stop codon (Supplemental Figures 2C and 2D).

Next, we assessed *pru1*, *pho1-2*, a *WRKY6*-overexpressing line (*35S:WRKY6-9*), and wild-type plants for sensitivity to low-Pi stress. When grown on Pi-sufficient conditions (MS; MS medium with 1.25 mM Pi), no obvious phenotypic differences were

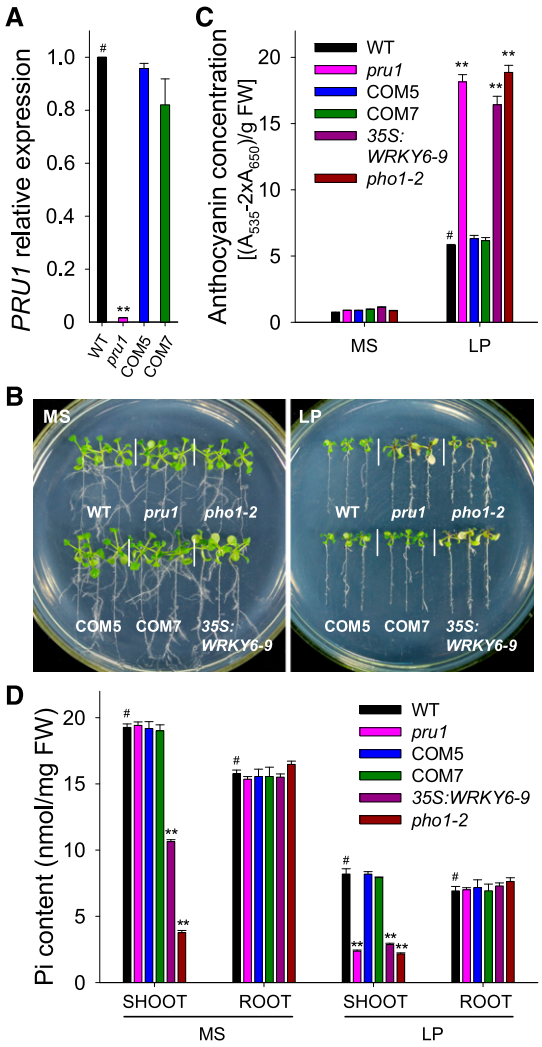


**Figure 1.** Phenotypic Comparison and Pi Contents among Various Genotypes.

**(A)** Analysis of *PRU1* expression in the *pru1* mutant, complementation lines (COM5 and COM7), and wild-type plants (WT) using RT-qPCR. Data are the mean values of three biological replicates ± SE.

**(B)** Phenotypic comparison. All genotypes were germinated and grown on MS medium for 7 d and then transferred to either MS medium or LP medium (LP, low-Pi medium containing 10 μM Pi) for another 7 d.

**(C)** Anthocyanin measurement. The 7-d-old seedlings were transferred to MS or LP medium for 7 d and then harvested for anthocyanin content measurements. The experiments were performed in biological triplicate, and 15 plants were measured in each replicate. FW, fresh weight.

**(D)** Pi content measurement. The 7-d-old seedlings were transferred to MS or LP medium for 5 d, the shoots and roots were harvested, and Pi content was measured. The experiments were conducted in biological triplicate, and a group of 15 seedlings was used as one biological sample.

Asterisks indicate significant differences compared with wild-type plants (#) by Student's *t* test: **P < 0.01.

observed among these genotypes (Figure 1B, left panel). When grown on Pi-deficient conditions (LP; low-Pi medium with 10 μM Pi), the *pru1* mutant exhibited increased sensitivity to low-Pi stress, similar to the *pho1-2* mutant and *WRKY6*-overexpressing line (*35S:WRKY6-9*) (Figure 1B, right panel). Complementation with *PRU1* rescued the increased low-Pi sensitivity of *pru1* (Figure 1B, right panel). Anthocyanin accumulation is one of the most striking symptoms of Pi starvation in plants. During Pi starvation, the *pru1* mutant, similar to *pho1-2* and *35S:WRKY6-9*, accumulated more anthocyanin than wild-type plants, while complementation lines contained similar amounts of anthocyanin as wild-type plants (Figure 1C).

Both the *pho1* mutant and the *WRKY6*-overexpressing lines are defective in Pi transfer from roots to shoots and concomitantly have reduced Pi contents in the shoot (Poirier et al., 1991; Hamburger et al., 2002; Chen et al., 2009). Consistent with this, the *pho1-2* mutant and *35S:WRKY6-9* line displayed significantly lower Pi contents in the shoot relative to wild-type plants under both Pi-sufficient and Pi-deficient conditions (Figure 1D). Although the shoot Pi content was reduced, the *pho1-2* mutant,

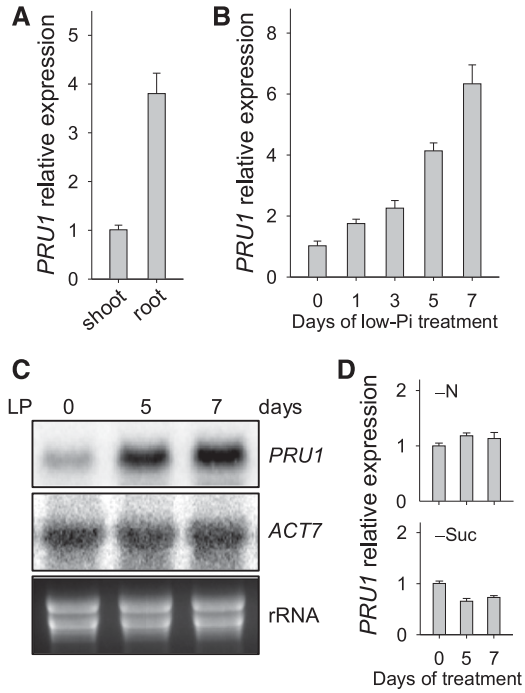


**Figure 2.** *PRU1* Expression Pattern.

**(A)** Analysis of *PRU1* expression in wild-type plants using RT-qPCR. The wild-type plants were germinated and grown on MS medium for 7 d, and the roots and shoots were harvested separately for RNA extraction. Data are mean values of three biological replicates ± SE.

**(B)** Analysis of *PRU1* expression during Pi starvation using RT-qPCR. The 7-d-old wild-type seedlings were transferred to LP medium and then the roots were harvested at the indicated time points for RNA extraction. Data are mean values of three biological replicates ± SE.

**(C)** Analysis of *PRU1* expression during Pi starvation using RNA gel blot analysis. Seven-day-old wild-type seedlings were transferred to LP medium, and the roots were harvested at the indicated time points for RNA extraction. *ACT7* and rRNA were used as loading controls.

**(D)** Analysis of *PRU1* expression under nitrogen or sucrose deficiency using RT-qPCR. The 7-d-old wild-type seedlings were transferred to –N or –Suc medium, and then the roots were harvested at the indicated time points for RNA extraction. Data are mean values of three biological replicates ± SE.

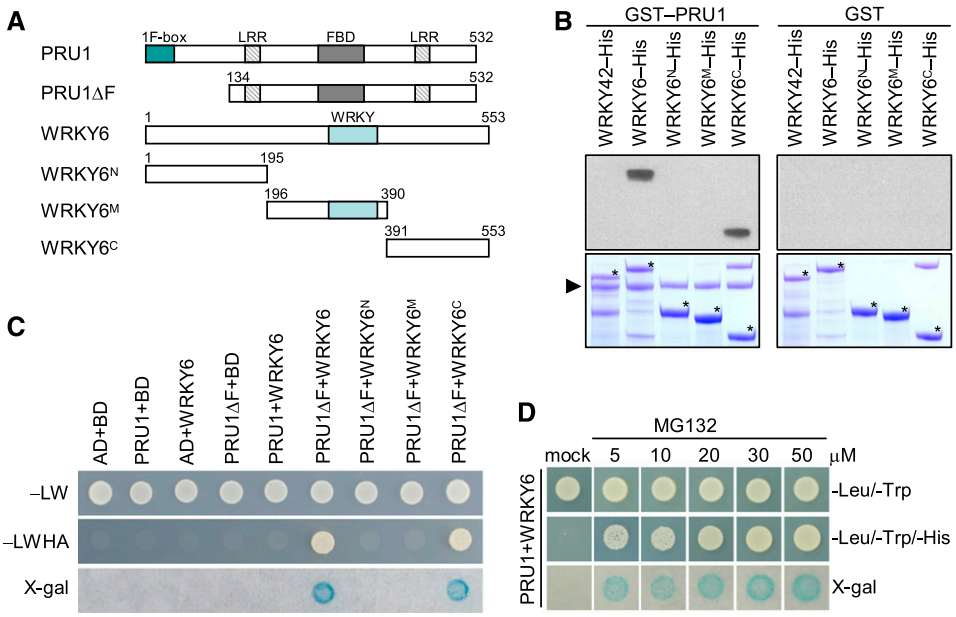


**Figure 3.** Interaction between PRU1 and WRKY6 in Vitro and in Yeast.

**(A)** Schematics of full-length PRU1, WRKY6, and their deletion derivatives. Numbers refer to the positions of the first or last amino acid in the sequences.
**(B)** In vitro pull-down assay of the interaction between recombinant PRU1 and WRKY6. GST-PRU1 and GST were used as baits, and WRKY42-His, WRKY6-His, WRKY6$^{N}$-His, WRKY6$^{M}$-His, and WRKY6$^{C}$-His were used as targets. The bound proteins were analyzed by immunoblotting using an anti-His antibody. The triangle indicates GST-PRU1, and asterisks indicate the target proteins.
**(C)** Interaction between PRU1 and WRKY6 in a yeast two-hybrid assay. Yeast cells were grown on control medium (SD/-Leu/-Trp [−LW]) or selective medium (SD/-Leu/-Trp/-His/-Ade [−LWHA]).
**(D)** Interaction between PRU1 and WRKY6 in a yeast two-hybrid assay with MG132 in DMSO, or DMSO only (mock).

similar to the *PHO1*-underexpressing lines, showed normal plant growth at the early seedling stage under Pi-sufficient conditions (Figures 1B and 1D; Rouached et al., 2011). Rouached et al. (2011) demonstrated that the retarded growth of the mature *pho1-2* mutant was not a direct consequence of Pi deficiency, but was due to extensive gene expression reprogramming triggered by Pi deficiency (Rouached et al., 2011).

The *pru1* mutant had similar levels of Pi in the shoot as wild-type plants under Pi-sufficient conditions, whereas the same line grown under Pi-deficient conditions had reduced Pi contents in the shoot, similar to what was observed for the *pho1-2* and *35S:WRKY6-9* (Figure 1D). Pi levels were restored to wild-type levels in the shoots of the COM5 and COM7 complementation lines (Figure 1D). These data demonstrate that Arabidopsis PRU1 modulates Pi transfer from roots to shoots under low-Pi stress.

### *PRU1* Expression Pattern

Consistent with the function of root-to-shoot Pi transfer, *PRU1* was primarily expressed in the roots (Figure 2A). To measure the transcript abundance of *PRU1* in wild-type roots during Pi starvation, 7-d-old plants were transferred to LP medium and then the roots were harvested at the indicated time points. During Pi starvation, the transcript abundance of *PRU1* was enhanced (Figures 2B and 2C). The transcript abundance of *PRU1* was not induced by nitrogen deficiency and was slightly reduced in the absence of sucrose (Figure 2D).

### PRU1 Interacts with WRKY6 in Vitro and in Yeast

Similar to *35S:WRKY6-9*, the *pru1* mutant was sensitive to low-Pi stress and had reduced levels of Pi in the shoot under Pi-deficient conditions (Figure 1). Therefore, we hypothesized that the PRU1 may reduce WRKY6 accumulation during Pi starvation. First, we tested for an interaction between PRU1 and WRKY6. The predicted PRU1 protein was composed of 532 amino acids, containing an F-box domain at the N terminus, two LRR domains, and an FBD domain (Figure 3A). The F-box domain was identified as a protein-protein interaction motif that links F-box proteins to the core of the SKP1-Cullin-F-box (SCF) complex by interacting with SUPPRESSOROF KINETOCHORE PROTEIN1 (SKP1) (Bai et al., 1996). The LRR domain consisted of 20 to 30 amino acids that generally fold into a horseshoe shape (Enkhbayar et al., 2004) and appears to provide the structural framework for protein-protein interactions (Kobe and Kajava, 2001). The FBD domain is reported in F-box proteins as well as other domain-containing plant proteins and is proposed to be associated with nuclear processes (Doerks et al., 2002). To test for an interaction between PRU1 and WRKY6, WRKY6 was cleaved into three fragments, WRKY6$^{N}$, WRKY6$^{M}$, and WRKY6$^{C}$ (Figure 3A). The recombinant fusion proteins PRU1, WRKY6, and WRKY6 derivates were purified from *Escherichia coli*

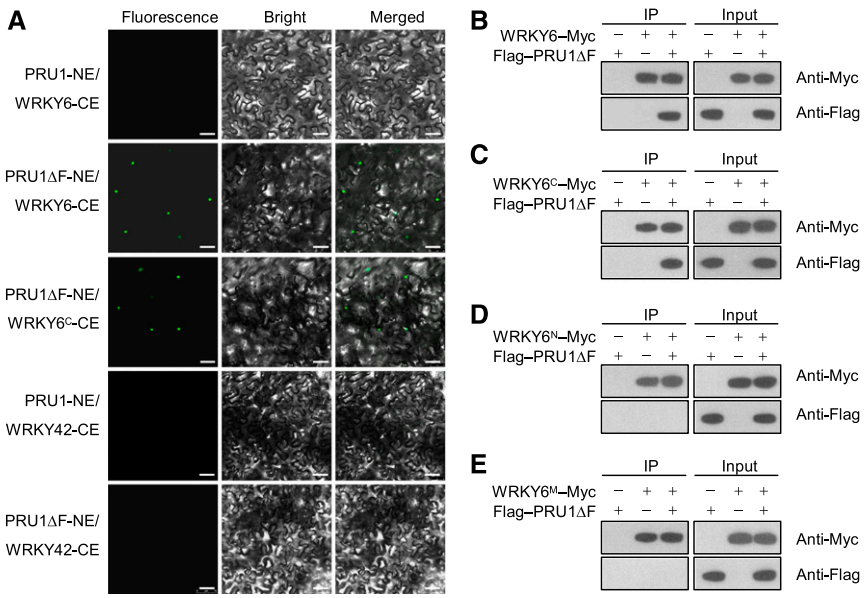


**Figure 4.** Interaction between PRU1 and WRKY6 in Vivo.

**(A)** BiFC analysis of the interaction between PRU1 and WRKY6 in *N. benthamiana* leaves. Bars = 50 μm.
**(B)** to **(E)** Coimmunoprecipitation assay for PRU1ΔF and WRKY6 in Arabidopsis protoplasts. The *Flag-PRU1ΔF* construct was transiently coexpressed with *WRKY6-Myc* **(B)**, *WRKY6$^{C}$-Myc* **(C)**, *WRKY6$^{N}$-Myc* **(D)**, or *WRKY6$^{M}$-Myc* **(E)** in Arabidopsis protoplasts. Protein extracts were immunoprecipitated with an anti-Myc affinity gel matrix. Input proteins and immunoprecipitates (IP) were analyzed by immunoblotting using anti-Myc and anti-Flag antibodies.

and used in pull-down assays. As shown in Figure 3B, the recombinant GST-PRU1 bound to WRKY6 as well as the C terminus of WRKY6 (WRKY6$^{C}$), but not to WRKY6$^{N}$, WRKY6$^{M}$, or WRKY42, which is a close homolog of WRKY6 (Eulgem et al., 2000).

We also tested for an interaction between PRU1 and WRKY6 using a yeast two-hybrid system; however, full-length PRU1 failed to interact with WRKY6 in yeast (Figure 3C). Within the SCF complex, the F-box protein determines the specificity of the complex. The F-box protein contains at least two domains: an F-box domain, which binds to SKP1, and a protein-protein interaction domain, which determines the substrate specificity of the SCF complex (Lechner et al., 2006). We hypothesized that the interaction between PRU1 and WRKY6 resulted in the degradation of WRKY6. In agreement with this hypothesis, the interaction could not be detected in yeast. To investigate if PRU1 interacts with SKP1 through the F-box domain (Lechner et al., 2006), we generated a truncated version of PRU1 that lacks the F-box domain (PRU1ΔF, Figure 3A). The PRU1ΔF and WRKY6 transformants grew well on SD/-Leu/-Trp/-His/-Ade medium (−LWHA) and showed strong β-galactosidase activity (Figure 3C), indicating that PRU1ΔF interacted with WRKY6 in yeast. Consistent with the pull-down results, PRU1ΔF also bound to WRKY6$^{C}$ in yeast (Figure 3C). MG132, a proteasome inhibitor, can impair proteasome-mediated protein degradation in yeast (Ahuja et al., 2017). To further confirm the interaction between PRU1 and WRKY6 in yeast, MG132 in DMSO (5, 10, 20, 30, or 50 μM) or DMSO only (mock) was added into the media. As shown in Figure 3D, full-length PRU1 interacted with WRKY6 in yeast in the presence of MG132. These data demonstrate that PRU1 interacts with WRKY6 in vitro and in yeast.

## PRU1 Binds to WRKY6 in Vivo

We then tested for the interaction between PRU1 and WRKY6 in *Nicotiana benthamiana* using a bimolecular fluorescence complementation (BiFC) assay. *PRU1* and *PRU1ΔF* were cloned individually into the *pSPYNE173* vector (NE), and *WRKY6* and *WRKY6$^{C}$* were cloned individually into the *pSPYCEM* vector (CE), and then various combinations of these vectors were transiently coexpressed in *N. benthamiana* leaves. No fluorescence signals were observed when full-length PRU1 and WRKY6 were coexpressed, whereas a strong fluorescence signal was observed in the nucleus when PRU1ΔF and WRKY6, or PRU1ΔF and WRKY6$^{C}$ were coexpressed (Figure 4A). This indicates that PRU1 interacted with WRKY6 in the nucleus. Neither PRU1 nor PRU1ΔF interacted with WRKY42 in *N. benthamiana* leaves (Figure 4A).

A coimmunoprecipitation assay was also performed in Arabidopsis protoplasts to confirm the interaction between PRU1ΔF and WRKY6. The coimmunoprecipitation assays showed that Flag-PRU1ΔF coimmunoprecipitated with WRKY6-Myc (Figure 4B) and WRKY6$^{C}$-Myc (Figure 4C), but not with WRKY6$^{N}$-Myc (Figure 4D) or WRKY6$^{M}$-Myc (Figure 4E). This suggests that the C terminus of WRKY6 was essential for the interaction between WRKY6 and PRU1. Together, these data indicate that PRU1 binds to WRKY6 in vivo as well as in vitro.

## PRU1 Interacts with ASK Proteins and Modulates Polyubiquitination of WRKY6 in Vivo

The SCF complex is composed of Cullin1 (CUL1), SKP1, RING-BOX1 (RBX1), and an F-box protein. CUL1 interacts with RBX1 at

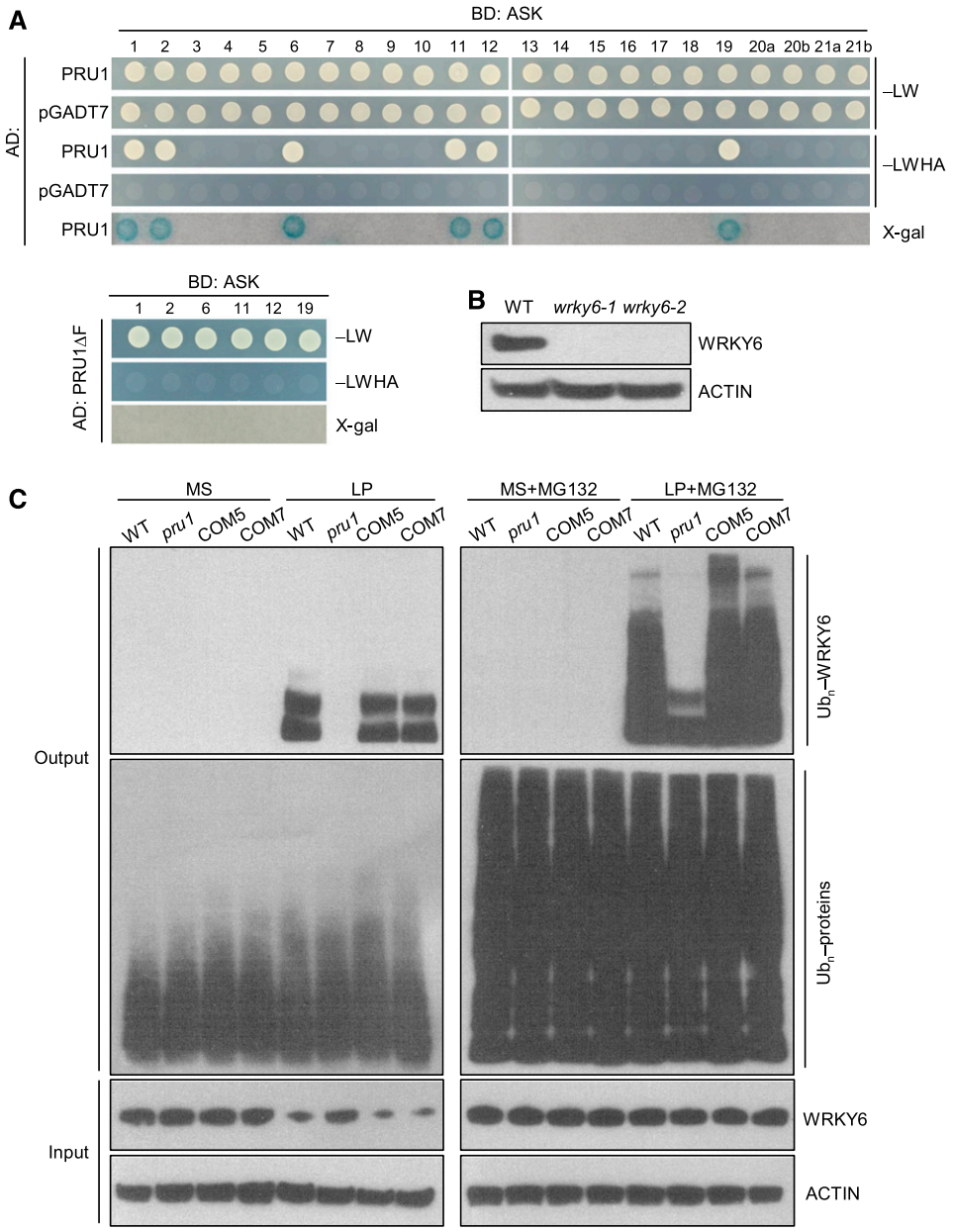


**Figure 5.** PRU1 Interacts with ASK Proteins and Modulates the Ubiquitination of WRKY6.

**(A)** Yeast two-hybrid assay testing for an interaction between PRU1 and multiple ASK proteins. The yeast cells were grown on control medium (SD/-Leu/-Trp [LW]) or selective medium (SD/-Leu/-Trp/-His/-Ade [LWHA]).

**(B)** Immunoblot analysis of WRKY6 protein in *wrky6* mutants (*wrky6-1* and *wrky6-2*) and wild-type plants with an anti-WRKY6 antibody. ACTIN was used as the loading control.

**(C)** Polyubiquitination of WRKY6 in the *pru1* mutant, complementation lines, and wild-type plants. Seven-day-old seedlings were transferred to MS medium, LP medium, MS medium supplemented with 10 μM MG132 (MS+MG132), or LP medium supplemented with 10 μM MG132 (LP+MG132) for 3 d and then the roots were harvested and protein was extracted. Each total protein extract was incubated with a P62-agarose matrix to obtain ubiquitinated proteins. Polyubiquitinated WRKY6 was detected with an anti-WRKY6 antibody, and total ubiquitinated proteins were measured with an anti-Ub antibody in the Output. The accumulations of WRKY6 and ACTIN were tested in the Input.

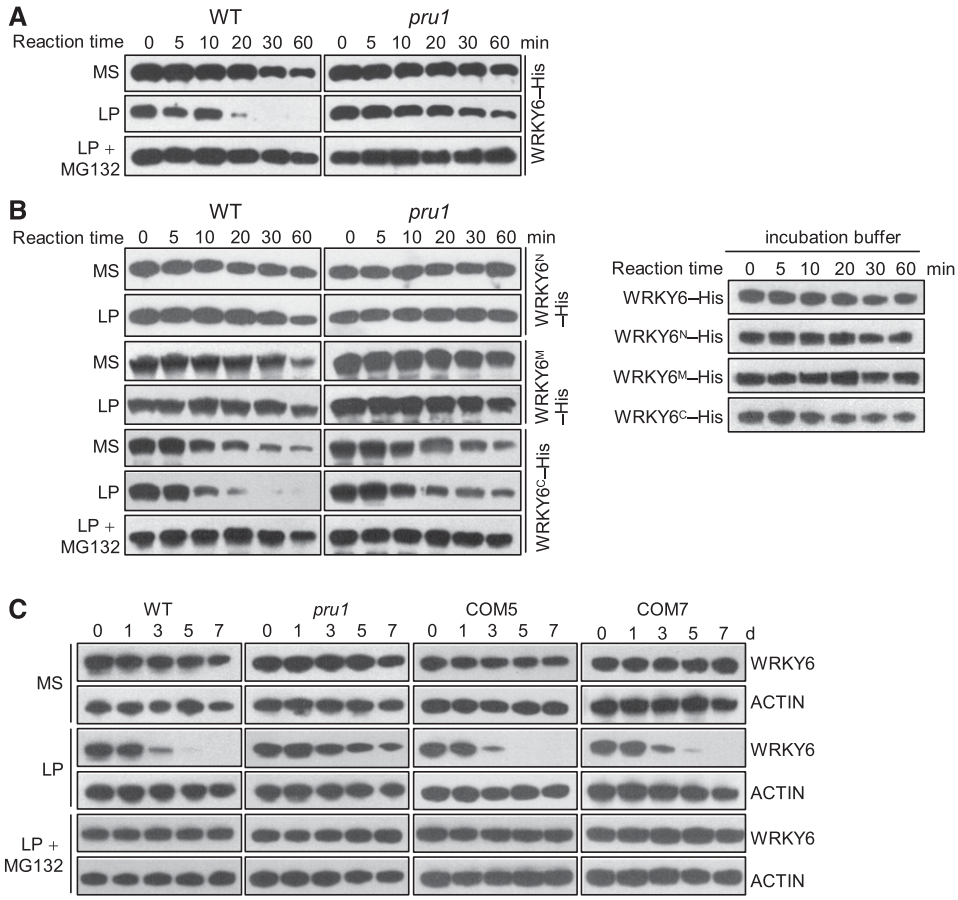


**Figure 6.** PRU1 Mediates WRKY6 Degradation Under Low-Pi Stress.

**(A)** and **(B)** Cell-free degradation assay. Seven-day-old *pru1* mutant and wild-type seedlings were transferred to MS medium, LP medium, or LP medium containing 10 μM MG132 for 3 d, and then the roots were harvested and protein was extracted. The root protein extracts were incubated with recombinant WRKY6-His **(A)** or its deletion derivatives ($WRKY6^N$-His, $WRKY6^M$-His, or $WRKY6^C$-His) **(B)** for the indicated periods, and the abundance of WRKY6 or its deletion derivatives was determined by immunoblotting with anti-His antibody. Recombinant WRKY6-His or its derivatives in incubation buffer (without root proteins) were used as controls.

**(C)** Immunoblot analysis of WRKY6 in the *pru1* mutant, complementation lines (COM5 and COM7) and wild-type plants. Seven-day-old seedlings were transferred to MS medium, LP medium, or LP medium containing 10 μM MG132, and then the roots were harvested at the indicated time points and protein was extracted. The abundance of WRKY6 was analyzed by immunoblotting using an anti-WRKY6 antibody. ACTIN was used as the loading control.

its C terminus and SKP1 at its N terminus, which in turn binds to the F-box protein (Lechner et al., 2006). In Arabidopsis, the ARABIDOPSIS SKP1-like (ASK) protein interacts with CUL1 and the F-box protein to function as an SCF E3 ubiquitin ligase (Lechner et al., 2006). There are 23 ASK proteins in the Arabidopsis genome (Risseeuw et al., 2003). To examine whether PRU1 was a component of an SCF complex, we tested for interactions between PRU1 and various ASKs using the yeast two-hybrid assay. Among the 23 Arabidopsis ASK proteins, PRU1 interacted with ASK1, 2, 6, 11, 12, and 19 (Figure 5A), while truncated PRU1 lacking the F-box domain (PRU1ΔF) did not interact with any of these six ASK proteins (Figure 5A). Not all six ASK proteins showed close phylogenetic relationships (Supplemental Figure 3A), whereas there were several conserved amino acids among these six ASK proteins (Supplemental Figure 3B), suggesting that these conserved amino acids influenced the specificity of physical interactions between PRU1 and ASK proteins.

Furthermore, the polyubiquitination of WRKY6 was assessed in the *pru1* mutant, complementation lines, and wild-type plants. Seven-day-old seedlings were transferred to MS medium, LP medium, MS medium supplemented with 10 μM MG132 (MS+MG132), or LP medium supplemented with 10 μM MG132 (LP+MG132) for 3 d and then the roots were harvested for protein extraction. The proteasome inhibitor MG132 was added to block the degradation of ubiquitinated proteins, and the ubiquitinated proteins were enriched with P62-agarose. Polyubiquitinated WRKY6 was detected by immunoblotting with an anti-WRKY6 antibody that was known to be specific since signals corresponding to the same size of WRKY6 were not detected in two *wrky6* mutants, whereas they were in wild-type plants (Figure 5B).

Under Pi-sufficient conditions (MS or MS+MG132), no polyubiquitination signal of WRKY6 was detected among the various genotypes (Figure 5C). When grown under low-Pi stress (LP), WRKY6 was polyubiquitinated in the wild-type plants and complementation lines (COM5 and COM7), and no WRKY6 polyubiquitination signal was visible in the *pru1* mutant (Figure 5C). Furthermore, when grown under LP+MG132 conditions, the WRKY6 polyubiquitination signal was markedly higher in the wild-type plants and complementation lines than in the *pru1* mutant (Figure 5C). The ubiquitination signals of total ubiquitinated proteins were similar among all genotypes under Pi-sufficient or Pi-deficient conditions (Figure 5C). The accumulation of WRKY6 was also assessed in the same plants at the same time points. When grown under low-Pi conditions, the accumulation of WRKY6 was reduced in wild-type plants and complementation lines, and the *pru1* mutant showed a relatively high level of WRKY6 protein compared with wild-type plants (Figure 5C). These data indicate that PRU1 ubiquitinates WRKY6 under low-Pi stress.

### PRU1 Modulates WRKY6 Degradation during Pi Starvation

We next compared WRKY6 protein levels in the *pru1* mutant and wild-type plants using a cell-free degradation assay. The 7-d-old seedlings were transferred to MS, LP, or LP+MG132 media for 3 d and then roots were collected for protein extraction. When WRKY6-His was incubated with the total proteins from plants grown on MS medium, no differences were detected in the abundance of WRKY6-His between *pru1* and wild-type plants (Figure 6A). When incubated with total proteins from plants grown on LP medium, the abundance of WRKY6-His was distinctly reduced in wild-type plants, whereas WRKY6-His levels remained relatively high in the *pru1* mutant (Figure 6A). Additionally, this low-Pi-induced reduction of WRKY6-His was inhibited by MG132 (Figure 6A). Since PRU1 interacted with the C terminus of WRKY6 ($WRKY6^C$, Figures 3 and 4), we also measured the protein levels of WRKY6 derivatives using a cell-free degradation system. When incubated with the total proteins from wild-type plants grown on LP medium, only $WRKY6^C$-His showed a low-Pi-induced decrease, which was impaired in the *pru1* mutant (Figure 6B). The abundance of recombinant WRKY6 proteins was reduced when incubated with root proteins from plants grown on MS medium, similar to those incubated with incubation buffer (without root proteins) (Figures 6A and 6B), indicating that the cell-free incubation buffer influenced the stability of recombinant WRKY6.

Furthermore, the protein level of WRKY6 was analyzed among the *pru1* mutant, complementation lines, and wild-types plants by immunoblotting with anti-WRKY6 antibody. The 7-d-old seedlings were transferred to MS, LP, or LP+MG132 medium, and the roots were harvested at the indicated time points. Consistent with a previous report, WRKY6 was degraded in wild-type roots during Pi starvation, and this degradation was inhibited by adding MG132 (Figure 6C; Chen et al., 2009). By contrast, the low-Pi-induced degradation of WRKY6 was reduced in the *pru1* mutant (Figure 6C), and normal degradation of WRKY6 was restored in the complementation lines (COM5 and COM7) (Figure 6C).

Our previous report showed that WRKY6 directly downregulates *PHO1* expression under Pi-sufficient conditions and that WRKY6 is degraded under low-Pi stress, releasing its repression of *PHO1* (Chen et al., 2009). Therefore, we assessed the abundance of *PHO1* transcripts among *pru1*, complementation lines, and wild-type plants. During Pi starvation, the *PHO1* transcript abundance was enhanced in wild-type plants (Figure 7; Stefanovic et al., 2007; Ribot et al., 2008; Chen et al., 2009), whereas this increase was significantly reduced in the *pru1* mutant (Figure 7). The *PHO1* transcript abundance in COM5 and COM7 was similar to that in wild-type plants (Figure 7). These results suggest that PRU1 modulates the degradation of WRKY6 in response to low-Pi stress.

### The *35S:WRKY6* and *pru1 35S:WRKY6* Lines Display Similar Phenotypes in Response to Pi Starvation

To evaluate the relationship between PRU1 and WRKY6, we generated the *pru1 35S:WRKY6* line by crossing *pru1* with *35S:WRKY6-9* (Figure 8A). The *35S:WRKY6-9* and *pru1 35S:WRKY6* lines accumulated more WRKY6 protein than either the *pru1* mutant or wild-type plants under Pi-sufficient or Pi-deficient conditions (Figure 8B). When grown on LP medium, the *pru1*, *35S:WRKY6-9*, and *pru1 35S:WRKY6-9* lines displayed similar low-Pi sensitive phenotypes (Figure 8C). Under Pi-sufficient conditions (MS medium), the *pru1* mutant had a similar level of Pi in the shoot as wild-type plants, whereas the *pru1 35S:WRKY6* line had reduced levels of Pi in the shoot, similar to *35S:WRKY6-9* (Figure 8D). Under low-Pi stress, the *pru1*, *pho1-2*, *35S:WRKY6-9*, and *pru1 35S:WRKY9* lines had significantly less Pi in the shoots compared with wild-type plants (Figure 8D).

Since WRKY6 influenced the expression of *PHO1*, we also assessed *PHO1* expression in these lines. Under Pi-sufficient conditions, the *PHO1* transcript abundance was significantly lower in

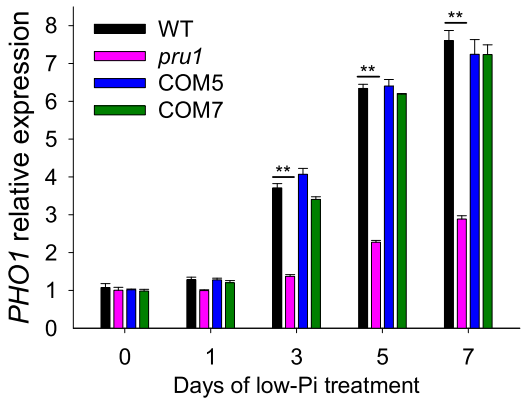


**Figure 7.** Analysis of *PHO1* Expression by RT-qPCR in the *pru1* Mutant, Complementation Lines (COM5 and COM7), and Wild-type Plants during Pi Starvation.

Seven-day-old seedlings were transferred to LP medium and the roots were harvested at the indicated time points for RNA extraction. Data are mean values of three biological replicates ± SE. Asterisks indicate statistically significant differences compared with wild-type plants by Student's *t* test: **$P < 0.01$.

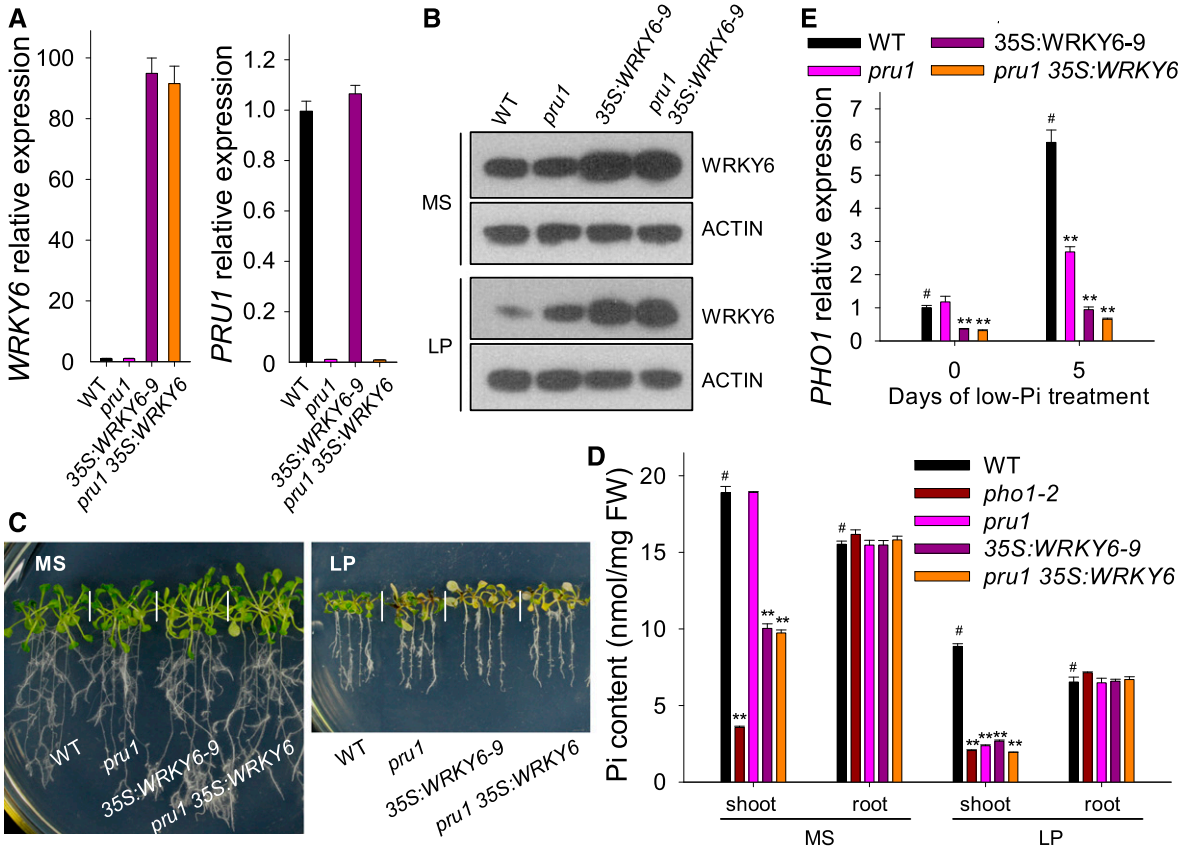


**Figure 8.** The *pru1 35S:WRKY6* Line Shows a Similar Phenotype to the *35S:WRKY6-9* Line.

**(A)** Analysis of transcript abundance of *WRKY6* and *PRU1* in the *pru1* mutant, *WRKY6*-overexpressing line (*35S:WRKY6-9*), *pru1 35S:WRKY6* line, and wild-type plants by RT-qPCR. Data are mean values of three biological replicates ± SE.

**(B)** Immunoblot analysis of WRKY6 in the *pru1* mutant, *35S:WRKY6-9*, *pru1 35S:WRKY6* line, and wild-type plants. Seven-day-old seedlings were transferred to MS or LP medium for 3 d, and then the roots were harvested and protein was extracted. The abundance of WRKY6 was analyzed using an anti-WRKY6 antibody. ACTIN was used as the loading control.

**(C)** Phenotypic comparison of various genotypes. Seven-day-old seedlings were transferred to MS or LP media for 7 d, and then photographs were taken.

**(D)** Pi content measurement. Seven-day-old plants were transferred to MS or LP media for 5 d, and then the shoots and roots were harvested for Pi content measurements. Three biological replicates were performed, and a group of 15 seedlings was pooled for each biological sample. Data are mean values of three biological replicates ± SE.

**(E)** Analysis of *PHO1* expression by RT-qPCR. Seven-day-old plants of various genotypes were transferred to LP medium, and the roots were harvested at the indicated time points for RNA extraction. Data are mean values of three biological replicates ± SE. Asterisks in **(D)** and **(E)** indicate significant differences compared with wild-type plants (#) by Student's *t* test: **$P < 0.01$.

*pru1 35S:WRKY9* and *35S:WRKY6-9* lines than in wild-type plants, whereas the *pru1* mutant had a similar *PHO1* transcript abundance to wild-type plants (Figure 8E). During Pi starvation, the low-Pi-induced accumulation of *PHO1* expression was reduced in *pru1*, *35S:WRKY6-9*, and *pru1 35S:WRKY6* plants, while the repression of *PHO1* in *pru1 35S:WRKY6* was similar to that in *35S:WRKY6-9* (Figure 8E). These data suggest that PRU1 targets WRKY6 to mediate Pi transfer from roots to shoots.

### Disruption of *WRKY6* Rescues the Low-Pi Sensitivity of *pru1*

To provide direct evidence that the enrichment of WRKY6 was responsible for the reduced Pi contents in the shoot and reduced *PHO1* expression in the *pru1* mutant, we generated the *pru1 wrky6* double mutant by crossing *pru1* with *wrky6-2* (Figure 9A). There were no obvious differences among the various genotypes under Pi-sufficient conditions (Figure 9B, left panel). However, when plants were grown on LP medium, the *pru1* mutant displayed a low-Pi-sensitive phenotype that was similar to *pho1-2*, while the *pru1 wrky6* double mutant did not (Figure 9B, right panel). Furthermore, we measured the Pi contents in the shoots and roots of these lines. When grown on MS medium, only the *pho1-2* mutant had lower Pi content in the shoot among all tested genotypes (Figure 9C). Under low-Pi stress, the *pru1* mutant had a significantly reduced Pi content in the shoot, similar to *pho1-2*. This was restored in the *pru1 wrky6* double mutant (Figure 9C).

In agreement with these results, the low-Pi-induced accumulation of *PHO1* transcript was repressed in the *pru1* mutant, whereas

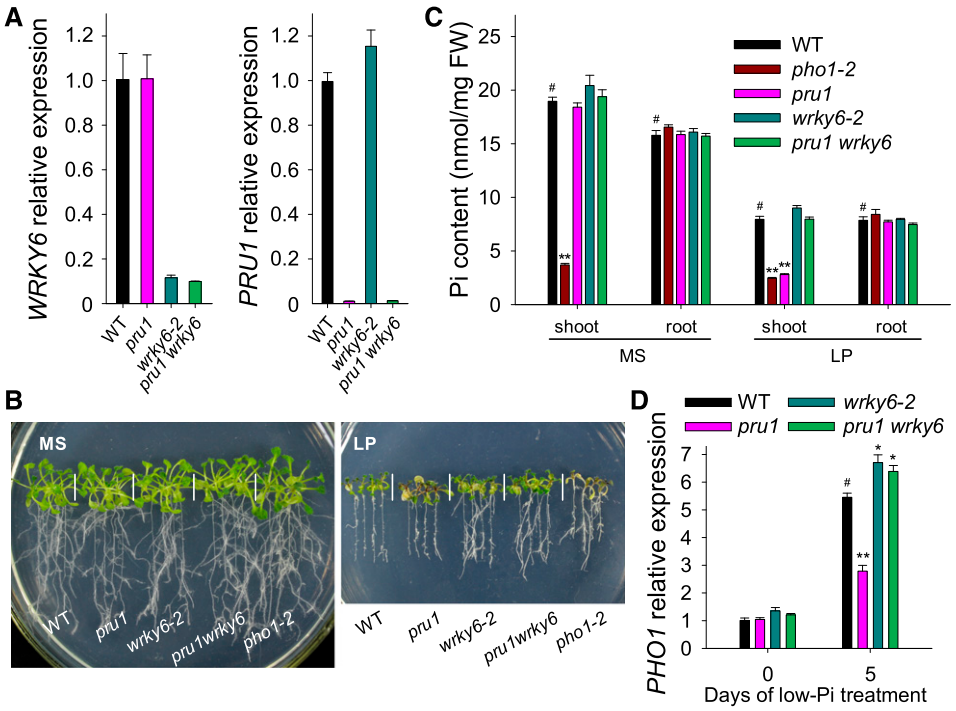


**Figure 9.** Disruption of *WRKY6* Rescues the Low-Pi Sensitivity of the *pru1* Mutant.

**(A)** Analysis of transcript abundance for *WRKY6* and *PRU1* in *pru1*, *wrky6-2*, *pru1 wrky6*, and wild-type plants using RT-qPCR. Data are mean values of three biological replicates ± SE.

**(B)** Phenotype comparisons. All genotypes were germinated and grown on MS medium for 7 d and then transferred to MS or LP medium for another 7 d.

**(C)** Pi content measurements. Seven-day-old plants were transferred to MS or LP medium and grown for an additional 5 d, and then the shoots and roots were harvested separately for Pi content measurement. Three biological replicates were performed, and a group of 15 seedlings was pooled for each biological sample. Data are mean values of three biological replicates ± SE.

**(D)** Analysis of *PHO1* expression by RT-qPCR. Seven-day-old plants and wild-type plants were transferred to LP medium, and then the roots were harvested at the indicated time points for RNA extraction. Data are mean values of three biological replicates ± SE. Asterisks in the **(C)** and **(D)** indicate significant differences compared with wild-type plants (#) by Student's *t* test: *P < 0.05; **P < 0.01.

the *pru1 wrky6* double mutant had slightly higher *PHO1* transcript abundance compared with wild-type plants under Pi-deficient conditions, similar to our observations of the *wrky6-2* mutant (Figure 9D). These results indicate that PRU1 modulates Pi transfer by controlling the degradation of WRKY6 under low-Pi stress.

### PUR1 Does Not Modulate the Degradation of WRKY42

WRKY42, a homolog of WRKY6, is also degraded via the ubiquitin 26S proteasome pathway during Pi starvation (Su et al., 2015). We therefore hypothesized that PRU1 also modulated the degradation of WRKY42. WRKY42 overexpression resulted in a decrease in *PHO1* expression and an increase in *PHT1;1* expression, which led to an elevated Pi content in the root (Su et al., 2015). The *pru1* mutant did not display an increase in Pi content in the root or in *PHT1;1* expression compared with wild-type plants under either Pi-sufficient or Pi-deficient conditions (Figures 1D and 10A). The low-Pi-induced degradation of WRKY42 in the *pru1* mutant was also similar to that in wild-type plants (Figure 10B). These data demonstrate that the low-Pi-induced degradation of WRKY42 is not modulated by PRU1, but by another E3 ligase.

## DISCUSSION

### The PRU1/WRKY6/PHO1-Regulatory Pathway Maintains Pi Homeostasis in Plants

Arabidopsis PHO1 plays an important role in Pi transfer from roots to shoots (Poirier et al., 1991; Hamburger et al., 2002), and the transcript abundance of *PHO1* increases significantly during Pi starvation (Stefanovic et al., 2007; Ribot et al., 2008; Chen et al., 2009). The transcription factor WRKY6 directly downregulates *PHO1* expression by binding to the W-boxes within the *PHO1* promoter under Pi-sufficient conditions. During Pi starvation, WRKY6 is degraded by the ubiquitin/26S proteasome pathway (Chen et al., 2009), suggesting that a ubiquitin E3 ligase(s) participates in modulating Pi homeostasis in response to low-Pi stress.

To identify the ubiquitin E3 ligase involved in WRKY6 degradation, we assessed ~400 T-DNA insertion mutants of putative E3 ligases for enhanced low-Pi sensitivity. The *pru1* mutant showed an enhanced low-Pi sensitive phenotype and had reduced Pi levels in the shoot under low-Pi stress, and complementation with *PRU1* restored these to wild-type levels (Figure 1), indicating that

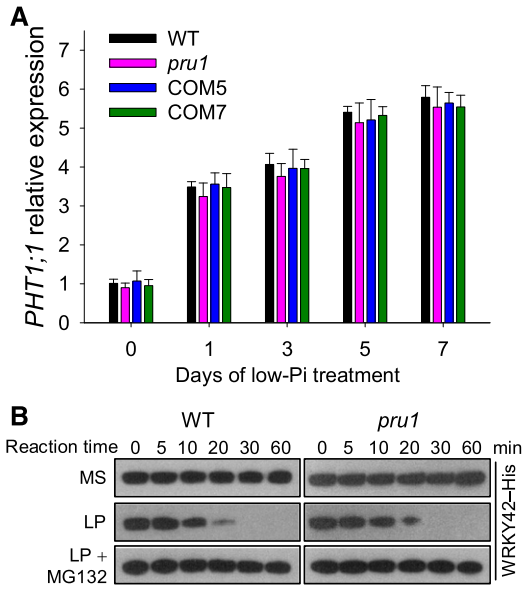


**Figure 10.** Analysis of *PHT1;1* Expression and WRKY42 Protein Content in the *pru1* Mutant and Wild-Type Plants.

**(A)** Analysis of *PHT1;1* expression in *pru1*, complementation lines, and wild-type plants during Pi starvation using RT-qPCR. Seven-day-old seedlings were transferred to LP medium, and the roots were harvested at the indicated time points. Data are mean values of three biological replicates ± SE ($n$ = 3).

**(B)** Cell-free degradation of WRKY42 in *pru1* and wild-type plants. Seven-day-old seedlings were transferred to MS, LP, or LP+MG132 medium and grown for an additional 3 d. The roots were harvested for a cell-free degradation assay. The root protein extracts were incubated with recombinant WRKY42-His for the indicated periods, and the abundance of WRKY42 was determined by immunoblotting with anti-His antibody.

PRU1 is involved in modulating Pi homeostasis under low-Pi stress. PRU1 targets WRKY6 in vitro and in vivo (Figures 3 and 4). Further biochemical evidence demonstrated that PRU1 mediates the ubiquitination and degradation of WRKY6 under low-Pi stress (Figures 5 and 6). In addition, disruption of *WRKY6* rescued the reduced Pi contents in the shoot and the repressed *PHO1* transcript abundance of the *pru1* mutant during Pi starvation (Figure 9), indicating that *WRKY6* was epistatic to *PRU1*. In conclusion, these data show that the PRU1/WRKY6/PHO1-regulatory pathway plays an important role in the plant's response to low-Pi stress. Under Pi-sufficient conditions, WRKY6 binds to W-box motifs within the *PHO1* promoter to repress *PHO1* expression, while under Pi-deficient conditions, PRU1 targets and ubiquitinates WRKY6 for proteasome-dependent degradation.

WRKY6 polyubiquitination was weak in the *pru1* mutant when grown on LP+MG132 medium compared with the wild type (Figure 5C), and low-Pi-induced degradation of WRKY6 was still observed in the *pru1* mutant (Figure 6C). This suggests that besides PRU1, other E3 ligases also modulate the degradation of WRKY6. The Arabidopsis genome did not contain a close homolog of PRU1; however, three F-box/RNI-like/FBD-like domain-containing proteins, encoded by AT3G58960, AT1G21990, and AT1G48400, were relatively close to PRU1 on the phylogenetic tree (Supplemental Figure 1A). We obtained the T-DNA insertion mutants for AT3G58960, AT1G21990, and AT1G48400 (Supplemental Data Set 1); however, no obvious low-Pi sensitivities were observed, indicating that these three F-box proteins did not play a major role in modulating the degradation of WRKY6.

Although WRKY42 is a close structural homolog of WRKY6, we found that PRU1 interacts with WRKY6, but not WRKY42 (Figures 3B and 4A). Furthermore, PRU1 cannot modulate the degradation of WRKY42 (Figure 10B). A pairwise sequence alignment was conducted between WRKY6 and WRKY42 using the Emboss Needle method (https://www.ebi.ac.uk/Tools/psa/emboss_needle/). The WRKY domain, an ~60-amino acid region, was highly conserved between WRKY6 and WRKY42 (Supplemental Figure 4). Three constructs were prepared with various WRKY6 fragments: $WRKY6^N$, $WRKY6^M$, and $WRKY6^C$ (Figure 3A). The $WRKY6^M$ fragment contained the conserved WRKYGQK domain and the $CX_7CX_{23}HXC$ zinc binding motif, which are required for proper DNA binding of WRKY proteins. The other two fragments, $WRKY6^N$ and $WRKY6^C$, were variable to WRKY42 (Supplemental Figure 4). We found that PRU1 interacts with $WRKY6^C$, but not $WRKY6^N$ or $WRKY6^M$ (Figures 3 and 4), suggesting that the $WRKY6^C$ fragment contains the sequence necessary for interaction with PRU1.

## PRU1-Dependent Posttranscriptional Regulation of WRKY6 Depends on Pi Levels

Posttranscriptional regulation is known to play important roles in plant Pi homeostasis under Pi-sufficient conditions. Together, the Arabidopsis E3 ubiquitin ligase NLA and the E2 ubiquitin conjugase PHO2 modulate the ubiquitination and subsequent degradation of Pi transporters under Pi-sufficient conditions (Lin et al., 2013; Park et al., 2014). Under Pi-sufficient conditions, the CK2$\alpha$3$\beta$3 protein kinase phosphorylates the PT8 Pi transporter, which inhibits localization of PT8 to the plasma membrane in rice (Chen et al., 2015). Recently, the SPX proteins AtSPX1/2 and OsSPX1/2 were reported to inhibit the transcription factors AtPHR1 and OsPHR2, respectively, under Pi-sufficient conditions (Puga et al., 2014; Wang et al., 2014).

Contrary to these reports, we found that PRU1 modulated the accumulation of WRKY6 mainly under Pi-deficient conditions. Our previous work showed that the *WRKY6* transcript abundance was not very responsive to Pi starvation, whereas the WRKY6 protein level was dramatically reduced during Pi starvation (Chen et al., 2009). This suggests that WRKY6 is primarily modulated at the posttranscriptional level in response to low-Pi stress. Further biochemical and molecular data showed that the PRU1 E3 ubiquitin ligase interacted with WRKY6 (Figures 3 and 4) to modulate its ubiquitination and subsequent degradation under low-Pi stress (Figures 5 and 6). This shows that PRU1 modulates the turnover of WRKY6 under Pi-deficient conditions. Although the *pru1* and *pho1-2* mutants showed similar low-Pi sensitive phenotypes and reduced Pi contents in the shoot under Pi-deficient conditions, there was an obvious difference in Pi content in the shoot between *pru1* and *pho1-2* when grown under Pi-sufficient conditions. The *pho1-2* mutant was a loss-of-function mutant and therefore displayed reduced Pi levels in the shoot under both Pi-sufficient and Pi-deficient conditions (Figure 1D; Poirier et al., 1991). However, the *pru1* mutant only displayed

reduced Pi levels in the shoot under Pi-deficient conditions, but not under Pi-sufficient conditions (Figure 1D), suggesting that PRU1 modulated Pi homeostasis primarily during Pi starvation.

Furthermore, when grown under Pi-sufficient conditions, no ubiquitination of WRKY6 was observed in either *pru1* mutant or wild-type plants, whereas when grown under Pi-deficient conditions, WRKY6 ubiquitination was observed in wild-type plants, while little to no WRKY6 ubiquitination was observed in the *pru1* mutant (Figure 5C). These data show that PRU1-mediated ubiquitination of WRKY6 depends on Pi supply levels. During Pi starvation, WRKY6 was significantly reduced in wild-type plants (Figure 6; Chen et al., 2009), and this degradation of WRKY6 was reduced in the *pru1* mutant (Figure 6), indicating that PRU1 modulated the low-Pi-induced degradation of WRKY6. Consequently, the *pru1* mutant had a reduced Pi content in the shoot and reduced *PHO1* transcript abundance compared with wild-type plants under low-Pi stress, yet there were no obvious differences between the *pru1* mutant and wild-type plants when grown on Pi-sufficient conditions (Figure 1). Together, these data demonstrate that the posttranscriptional regulation of WRKY6 by PRU1 depends on Pi levels.

Under Pi-sufficient conditions, the *PRU1* was expressed (Figures 2B and 2C), whereas the ubiquitination signal of WRKY6 was not observed (Figure 5C). Also, the ubiquitinated WRKY6 was significantly accumulated in wild-type plants under Pi-deficient conditions (Figure 5C). These data suggest that PRU1 is inactive under Pi-sufficient conditions, and is activated by posttranslational modification during Pi starvation. Several E3 ligases have been reported to be phosphorylated. For instance, the SnRK2.6 kinase phosphorylates the CHY ZINC-FINGER AND RING PROTEIN1 RING-finger E3 ligase (Ding et al., 2015), and the PUB12/13 U-box E3 ligases are phosphorylated by the BRASSINOSTEROID-INSENSITIVE1 kinase (Lu et al., 2011). In humans, the ATAXIA-TELANGIECTASIA MUTATED kinase phosphorylates the MURINE DOUBLE MINUTE2 E3 ligase to inhibit E3 ligase activity (Cheng et al., 2011). By contrast, the activity of the human Cb1-b (CASITAS B-LINEAGE LYMPHOMA-B) E3 ligase is activated by phosphorylation (Kobashigawa et al., 2011). Several amino acid residues of PRU1 were predicated to be phosphorylated, and Thr-504 was shown to be phosphorylated under isoxabene treatment, and Tyr-500 was phosphorylated during nitrate starvation/nitrate resupply (PhosPhAt, http://phosphat.uni-hohenheim.de/phosphat.html?code=AT3G42770.1). We thus hypothesize that PRU1 is phosphorylated under low-Pi stress and that this phosphorylation activates its E3 ligase activity. The mechanism regulating PRU1 activity merits further investigation.

## METHODS

### Plant Materials and Growth Conditions

The Col-0 ecotype was used as wild-type *Arabidopsis thaliana* in this study. The T-DNA insertion line Salk_069673C (referred to as the *pru1* mutant) was ordered from ABRC (http://www.arabidopsis.org/abrc). The *pho1-2* mutant, *WRKY6*-overexpressing line (*35S:WRKY6-9*), and *wrky6-1* mutant were described previously (Robatzek and Somssich, 2001; Hamburger et al., 2002). The *wrky6-2* mutant (Salk_012997) was a T-DNA insertion mutant ordered from ABRC (Huang et al., 2016).

For the complementation lines, a 3599-bp DNA fragment containing the coding region of *PRU1* and a 2-kb fragment of a region upstream of the start codon of *PRU1* were cloned into the *pCAMBIA1300* vector, designated as *ProPRU1:PRU1*. The *ProPRU1:PRU1* construct was introduced into the *pru1* mutant by *Agrobacterium tumefaciens*-mediated transformation (Agrobacterium strain GV3101) using the floral-dip method (Clough and Bent, 1998), and homozygous single-copy lines were obtained.

For plant growth, the Arabidopsis seeds were surface sterilized, treated at 4°C for 72 h, and then germinated and grown on MS medium containing 3% (w/v) sucrose and 0.8% (w/v) agar at 22°C for a 16-h daily light period at 80 $\mu$mol $m^{-2}$ $s^{-1}$ (Philips; TLD 36W/865 cool daylight), unless otherwise indicated.

The LP (low-Pi) medium used for low-Pi stress treatment was made by modifying MS medium to contain 10 $\mu$M Pi and agar instead of agarose (Promega). For sucrose or nitrogen deficiency, −Suc medium was made by preparing MS medium without sucrose, and −N medium was prepared as described previously (Rubio et al., 2001).

### Pi Content Measurement

The 7-d-old seedlings were transferred to MS or LP medium for 5 d and then the shoots and roots were harvested. The Pi contents in these samples were quantified as described previously (Su et al., 2015). Each experiment was performed in triplicate, and a group of 15 seedlings was used as one biological sample. Three independent experiments were performed.

### Anthocyanin Measurement

The 7-d-old seedlings were transferred to MS or LP medium for 7 d and then harvested for anthocyanin measurement. Anthocyanin contents were determined as described previously (Su et al., 2015). Each experiment was performed in triplicate, and measurements from 15 plants were pooled for one replicate. Three independent experiments were performed.

### RT-qPCR

The RT-qPCR assay was conducted as described previously (Huang et al., 2016), using SYBR Green PCR Master Mix (Life Technologies) on a 7500 Real Time PCR System (Applied Biosystems). Relative quantitative results were calculated by normalization to *Actin2/8*. Each experiment was performed in biological triplicate, and a group of ~120 seedlings was used as one biological replicate. At least three independent experiments were performed. The primers used are listed in Supplemental Table 1.

### RNA Gel Blot Analysis

Seven-day-old wild-type seedlings were transferred to LP medium and then the roots were harvested at the indicated time points for RNA extraction. The RNA gel blot analysis was conducted as described before (Chen et al., 2009). Thirty micrograms of total RNA from roots was loaded per lane and subsequently transferred to a nylon membrane for hybridization. The probes were amplified by PCR using *PRU1*-specific primers (5′-ATGAATTGTCTTCCA-GATGAGC-3′ and 5′-GGATCCCATGACTTGTATAATGA-3′) and *ACT7*-specific primers (5′-CTCAGCACCTTCCAACAGATGTGGA-3′and 5′-CCAAAAAAATGAACCAAGGACCAAA-3′) as the templates. The probes were labeled with [$\alpha$-$^{32}$P]dCTP using random primer labeling reagents. The probes of *PRU1* and *ACT7* were hybridized to RNA gel blotted onto nylon membrane. The rRNA was used as a loading control.

### BiFC Assay

*PRU1* and the *PRU1* deletion derivative (*PRU1ΔF*) were cloned into the *pSPYNE173* vector (NE) (Waadt and Kudla, 2008), while *WRKY6*, *WRKY6$^C$*, and *WRKY42* were cloned into the *pSPYCEM* vector (CE) (Waadt and Kudla, 2008). Each pair of constructs was cotransformed into *Nicotiana benthamiana* leaves. Five days after infiltration, YFP

fluorescence signals were observed using a confocal laser scanning microscope (Leica sp5).

### Yeast Two-Hybrid Assay

*PRU1* and its deletion derivative (*PRU1ΔF*) were cloned into the *pGADT7* vector (AD), while *WRKY6*, *WRKY6* deletion derivatives, and the *ASK* genes were cloned into *pGBKT7* vector (BD). Each pair of constructs was co-transformed into yeast strain AH109 for the yeast two-hybrid assay. Transformants growing well on SD/-Leu/-Trp medium (−LW) were considered to be positive clones. Interactions between two proteins were determined by growing transformants on SD/-Leu/-Trp/-His/-Ade medium (−LWHA) for 4 d and quantifying β-galactosidase activity. The primers used are listed in Supplemental Table 1.

### Protein Expression and Antibody Generation

*PRU1* and its deletion derivatives were cloned into the *pGEX-4T-1* vector to generate GST fusion proteins. The *WRKY42*, *WRKY6*, and *WRKY6* deletion derivatives were cloned into the *pET30a* vector to generate His fusion proteins. The recombinant constructs were transformed into *Escherichia coli* strain BL21. The *E. coli* cells were induced with 0.2 mM IPTG overnight at 18°C and collected by centrifugation at 4000 rpm for 15 min at 4°C. The fusion proteins were purified with glutathione-sepharose or Ni-sepharose.

The polyclonal antibody against WRKY6 was generated by inoculating mice.

### Immunoblot Analysis

Total proteins were extracted according to Chen et al. (2009), and 100 μg of protein from each sample was separated on a 10% SDS-PAGE gel and transferred to a polyvinylidene fluoride membrane. The abundances of WRKY6 and ACTIN were detected with anti-WRKY6 and anti-actin antibodies, respectively.

### Cell-Free Degradation Assay

The cell-free degradation assay was conducted as described previously (Su et al., 2015). To monitor the degradation of recombinant WRKY6 or its deletion derivatives, 250 ng of each purified recombinant protein was incubated in 20 μL of root protein extract (50 μg) at 22°C for the indicated time periods. The abundance of WRKY6 or its deletion derivatives was analyzed by immunoblotting with an anti-His antibody (MBL; D291-3, lot 007).

### In Vitro Pull-Down Assay

Purified GST-PRU1 or GST protein was incubated with an equal volume of glutathione-sepharose (GE Healthcare) in binding buffer (200 mM NaCl, 10 mM $Na_2HPO_4$, 1.8 mM $KH_2PO_4$, 2.7 mM KCl, 1 mM PMSF, and 5 mM DTT) at 4°C for 2 h. The mixture was washed three times with buffer I (200 mM NaCl, 10 mM $Na_2HPO_4$, 2.7 mM KCl, and 1.8 mM $KH_2PO_4$) and then aliquoted into five equal parts. Equal amounts of purified WRKY42-His, WRKY6-His, WRKY6$^N$-His, WRKY6$^M$-His, and WRKY6$^C$-His were added to the mixture and incubated for 2 h at 4°C. The mixture was rinsed three times with buffer II (20 mM Tris, pH 8.0, 500 mM NaCl, and 100 mM Imidazole), and the bound proteins were boiled in 1× SDS loading buffer for 5 min and then examined by immunoblotting using an anti-His antibody.

### Coimmunoprecipitation Assay

Coimmunoprecipitation assays were conducted as described previously (Feng et al., 2014). The coding sequences of *WRKY6* and its deletion derivatives were cloned into the *pCAMBIA1307-6myc* vector yielding *WRKY6-Myc*, *WRKY6$^N$-Myc*, *WRKY6$^M$-Myc*, and *WRKY6$^C$-Myc*. The coding sequence of *PRU1ΔF* was cloned into the *pCAMBIA1307-3flag* vector, yielding *Flag-PRU1ΔF*. The *Flag-PRU1ΔF* vector was cotransformed with *WRKY6-Myc*, *WRKY6$^N$-Myc*, *WRKY6$^M$-Myc*, or *WRKY6$^C$-Myc* in Arabidopsis mesophyll protoplasts. After a 16-h incubation, total proteins were extracted from the protoplasts. The protoplast protein extract was incubated with anti-Myc agarose (Sigma-Aldrich) at 4°C for 2 h. The input proteins and immunoprecipitates were detected by immunoblotting with either anti-Myc (Sigma-Aldrich) or anti-Flag (MBL) antibodies.

### Purification of Ubiquitinated Protein

The 7-d-old *pur1* mutant, complementation lines, and wild-type seedlings were transferred to MS medium, LP medium, MS medium with 10 μM MG132 (MS+MG132), or LP medium with 10 μM MG132 (LP +MG132) for 3 d, and roots were harvested for total protein extraction. The ubiquitinated proteins were purified as described previously (Kong et al., 2015). Briefly, 100 mg of root proteins from each genotype that was grown on MS, LP, MS+MG132, or LP+MG132 medium was used in the assay. Total proteins were used as Input (2 mg), and the remaining proteins (98 mg total proteins) were incubated with P62-agarose (Enzo Life Sciences; cat. no. BML-UW9010-0500) to obtain ubiquitinated proteins. Ubiquitinated proteins were separated on a 6% SDS-PAGE gel. The ubiquitinated WRKY6 was detected with an anti-WRKY6 antibody, and total ubiquitinated proteins were detected with an anti-Ub antibody (Santa Cruz Biotechnology; cat. no. sc-8017) in the output. WRKY6 and ACTIN accumulation were measured in the input.

### Phylogenetic Tree Construction

Amino acid sequences from the F-box/FBD-like domain-containing genes or Arabidopsis *ASK* genes were aligned in Clustal Omega (https://www.ebi.ac.uk/Tools/msa/clustalo/) (Supplemental Files 1 to 3) with default parameters. The neighbor-joining phylogenetic tree was conducted in MEGA 5.2 (Tamura et al., 2011). The tree nodes were evaluated by bootstrap analysis with 1000 replicates and were shown in the phylogenetic trees.

### Accession Numbers

Sequence data from this article can be found in the EMBL/GenBank data libraries under the following accession numbers: *PRU1* (AT3G42770), *WRKY6* (AT1G62300), *PHO1* (AT3G23430), *WRKY42* (AT4G04450), *PHT1;1* (AT5G43350), *ACT2* (AT3G18780), *ACT8* (AT1G49240), *ACT7* (AT5G09810), *ASK1* (AT1G75950), *ASK2* (AT5G42190), *ASK3* (AT2G25700), *ASK4* (AT1G20140), *ASK5* (AT3G60020), *ASK6* (AT3G53060), *ASK7* (AT3G21840), *ASK8* (AT3G21830), *ASK9* (AT3G21850), *ASK10* (AT3G21860), *ASK11* (AT4G34210), *ASK12* (AT4G34470), *ASK13* (AT3G60010), *ASK14* (AT2G03170), *ASK15* (AT3G25650), *ASK16* (AT2G03190), *ASK17* (AT2G20160), *ASK18* (AT1G10230), *ASK19* (AT2G03160), *ASK20a* (AT2G45950.1), *ASK20b* (AT2G45950.2), *ASK21a* (AT3G61415.1), and *ASK21b* (AT3G61415.2).

### Supplemental Data

**Supplemental Figure 1.** Phylogenetic tree of the F-box/FBD-like domain-containing proteins.

**Supplemental Figure 2.** Phenotype and mutation site of the *pho1-2* mutant.

**Supplemental Figure 3.** Phylogenetic analysis of Arabidopsis ASK proteins.

**Supplemental Figure 4.** Pairwise sequence alignment of WRKY6 and WRKY42 using the emboss needle method.

**Supplemental Table 1.** Sequences of primers used in this study.

**Supplemental Data Set 1.** Analysis of putative *e3* mutants.

**Supplemental File 1.** Alignment used to produce the phylogenetic tree shown in Supplemental Figure 1A.

**Supplemental File 2.** Alignment used to produce the phylogenetic tree shown in Supplemental Figure 1B.

**Supplemental File 3.** Alignment used to produce the phylogenetic tree shown in Supplemental Figure 3.

## ACKNOWLEDGMENTS

We thank Yves Poirier for providing the *pho1-2* mutant and Imre E. Somssich for providing the *WRKY6*-overexpressing line (*35S:WRKY6-9*) and *wrky6-1* mutant. This work was supported by grants from the Ministry of Agriculture of China for transgenic research (No. 2016ZX08009002 to Y.-F.C.), the National Natural Science Foundation of China (No. 31670245 to Y.-F.C. and No. 31421062 to W.-H.W.), and the '111' Project of China (No. B06003 to W.-H.W.).

## AUTHOR CONTRIBUTIONS

Y.-F.C. and W.-H.W. designed the research. Q.Y., H.W., and T.S. performed the research. Y.-F.C. and Q.Y. analyzed the data and wrote the article. W.-H.W. revised the article.

Received November 2, 2017; revised February 27, 2018; accepted March 13, 2018; published March 22, 2018.

## REFERENCES

**Ahuja, J.S., Sandhu, R., Mainpal, R., Lawson, C., Henley, H., Hunt, P.A., Yanowitz, J.L., and Börner, G.V.** (2017). Control of meiotic pairing and recombination by chromosomally tethered 26S proteasome. Science **355:** 408–411.

**Arpat, A.B., Magliano, P., Wege, S., Rouached, H., Stefanovic, A., and Poirier, Y.** (2012). Functional expression of PHO1 to the Golgi and *trans*-Golgi network and its role in export of inorganic phosphate. Plant J. **71:** 479–491.

**Aung, K., Lin, S.I., Wu, C.C., Huang, Y.T., Su, C.L., and Chiou, T.J.** (2006). *pho2*, a phosphate overaccumulator, is caused by a nonsense mutation in a microRNA399 target gene. Plant Physiol. **141:** 1000–1011.

**Bai, C., Sen, P., Hofmann, K., Ma, L., Goebl, M., Harper, J.W., and Elledge, S.J.** (1996). SKP1 connects cell cycle regulators to the ubiquitin proteolysis machinery through a novel motif, the F-box. Cell **86:** 263–274.

**Bari, R., Datt Pant, B., Stitt, M., and Scheible, W.R.** (2006). PHO2, microRNA399, and PHR1 define a phosphate-signaling pathway in plants. Plant Physiol. **141:** 988–999.

**Chen, J., et al.** (2015). The rice CK2 kinase regulates trafficking of phosphate transporters in response to phosphate levels. Plant Cell **27:** 711–723.

**Chen, Y.F., Li, L.Q., Xu, Q., Kong, Y.H., Wang, H., and Wu, W.H.** (2009). The WRKY6 transcription factor modulates *PHOSPHATE1* expression in response to low Pi stress in *Arabidopsis.* Plant Cell **21:** 3554–3566.

**Cheng, Q., Cross, B., Li, B., Chen, L., Li, Z., and Chen, J.** (2011). Regulation of MDM2 E3 ligase activity by phosphorylation after DNA damage. Mol. Cell. Biol. **31:** 4951–4963.

**Chiou, T.J., and Lin, S.I.** (2011). Signaling network in sensing phosphate availability in plants. Annu. Rev. Plant Biol. **62:** 185–206.

**Clough, S.J., and Bent, A.F.** (1998). Floral dip: a simplified method for *Agrobacterium*-mediated transformation of *Arabidopsis thaliana.* Plant J. **16:** 735–743.

**Ding, S., Zhang, B., and Qin, F.** (2015). Arabidopsis RZFP34/CHYR1, a ubiquitin E3 ligase, regulates stomatal movement and drought tolerance via SnRK2.6-mediated phosphorylation. Plant Cell **27:** 3228–3244.

**Doerks, T., Copley, R.R., Schultz, J., Ponting, C.P., and Bork, P.** (2002). Systematic identification of novel protein domain families associated with nuclear functions. Genome Res. **12:** 47–56.

**Enkhbayar, P., Kamiya, M., Osaki, M., Matsumoto, T., and Matsushima, N.** (2004). Structural principles of leucine-rich repeat (LRR) proteins. Proteins **54:** 394–403.

**Eulgem, T., Rushton, P.J., Robatzek, S., and Somssich, I.E.** (2000). The WRKY superfamily of plant transcription factors. Trends Plant Sci. **5:** 199–206.

**Feng, C.Z., Chen, Y., Wang, C., Kong, Y.H., Wu, W.H., and Chen, Y.F.** (2014). Arabidopsis RAV1 transcription factor, phosphorylated by SnRK2 kinases, regulates the expression of *ABI3, ABI4*, and *ABI5* during seed germination and early seedling development. Plant J. **80:** 654–668.

**Hamburger, D., Rezzonico, E., MacDonald-Comber Petétot, J., Somerville, C., and Poirier, Y.** (2002). Identification and characterization of the Arabidopsis *PHO1* gene involved in phosphate loading to the xylem. Plant Cell **14:** 889–902.

**Huang, T.K., et al.** (2013). Identification of downstream components of ubiquitin-conjugating enzyme PHOSPHATE2 by quantitative membrane proteomics in *Arabidopsis* roots. Plant Cell **25:** 4044–4060.

**Huang, Y., Feng, C.Z., Ye, Q., Wu, W.H., and Chen, Y.F.** (2016). *Arabidopsis* WRKY6 transcription factor acts as a positive regulator of abscisic acid signaling during seed germination and early seedling development. PLoS Genet. **12:** e1005833.

**Kant, S., Peng, M., and Rothstein, S.J.** (2011). Genetic regulation by NLA and microRNA827 for maintaining nitrate-dependent phosphate homeostasis in *Arabidopsis.* PLoS Genet. **7:** e1002021.

**Kobashigawa, Y., Tomitaka, A., Kumeta, H., Noda, N.N., Yamaguchi, M., and Inagaki, F.** (2011). Autoinhibition and phosphorylation-induced activation mechanisms of human cancer and autoimmune disease-related E3 protein Cbl-b. Proc. Natl. Acad. Sci. USA **108:** 20579–20584.

**Kobe, B., and Kajava, A.V.** (2001). The leucine-rich repeat as a protein recognition motif. Curr. Opin. Struct. Biol. **11:** 725–732.

**Kong, L., Cheng, J., Zhu, Y., Ding, Y., Meng, J., Chen, Z., Xie, Q., Guo, Y., Li, J., Yang, S., and Gong, Z.** (2015). Degradation of the ABA co-receptor ABI1 by PUB12/13 U-box E3 ligases. Nat. Commun. **6:** 8630.

**Lechner, E., Achard, P., Vansiri, A., Potuschak, T., and Genschik, P.** (2006). F-box proteins everywhere. Curr. Opin. Plant Biol. **9:** 631–638.

**Lin, W.Y., Huang, T.K., and Chiou, T.J.** (2013). Nitrogen limitation adaptation, a target of microRNA827, mediates degradation of plasma membrane-localized phosphate transporters to maintain phosphate homeostasis in *Arabidopsis.* Plant Cell **25:** 4061–4074.

**Liu, T.Y., Huang, T.K., Tseng, C.Y., Lai, Y.S., Lin, S.I., Lin, W.Y., Chen, J.W., and Chiou, T.J.** (2012). PHO2-dependent degradation of PHO1 modulates phosphate homeostasis in *Arabidopsis.* Plant Cell **24:** 2168–2183.

**López-Arredondo, D.L., Leyva-González, M.A., González-Morales, S.I., López-Bucio, J., and Herrera-Estrella, L.** (2014). Phosphate nutrition: improving low-phosphate tolerance in crops. Annu. Rev. Plant Biol. **65:** 95–123.

**Lu, D., Lin, W., Gao, X., Wu, S., Cheng, C., Avila, J., Heese, A., Devarenne, T.P., He, P., and Shan, L.** (2011). Direct ubiquitination

of pattern recognition receptor FLS2 attenuates plant innate immunity. Science **332:** 1439–1442.

**Marschner, H.** (2012). Marschner's Mineral Nutrition of Higher Plants. (London: Academic Press).

**Miura, K., Rus, A., Sharkhuu, A., Yokoi, S., Karthikeyan, A.S., Raghothama, K.G., Baek, D., Koo, Y.D., Jin, J.B., Bressan, R.A., Yun, D.J., and Hasegawa, P.M.** (2005). The *Arabidopsis* SUMO E3 ligase SIZ1 controls phosphate deficiency responses. Proc. Natl. Acad. Sci. USA **102:** 7760–7765.

**Mudge, S.R., Rae, A.L., Diatloff, E., and Smith, F.W.** (2002). Expression analysis suggests novel roles for members of the Pht1 family of phosphate transporters in *Arabidopsis.* Plant J. **31:** 341–353.

**Okumura, S., Mitsukawa, N., Shirano, Y., and Shibata, D.** (1998). Phosphate transporter gene family of *Arabidopsis thaliana.* DNA Res. **5:** 261–269.

**Park, B.S., Seo, J.S., and Chua, N.H.** (2014). NITROGEN LIMITATION ADAPTATION recruits PHOSPHATE2 to target the phosphate transporter PT2 for degradation during the regulation of *Arabidopsis* phosphate homeostasis. Plant Cell **26:** 454–464.

**Poirier, Y., Thoma, S., Somerville, C., and Schiefelbein, J.** (1991). Mutant of Arabidopsis deficient in xylem loading of phosphate. Plant Physiol. **97:** 1087–1093.

**Puga, M.I., et al.** (2014). SPX1 is a phosphate-dependent inhibitor of Phosphate Starvation Response 1 in *Arabidopsis.* Proc. Natl. Acad. Sci. USA **111:** 14947–14952.

**Raghothama, K.G.** (1999). Phosphate acquisition. Annu. Rev. Plant Physiol. Plant Mol. Biol. **50:** 665–693.

**Ribot, C., Wang, Y., and Poirier, Y.** (2008). Expression analyses of three members of the *AtPHO1* family reveal differential interactions between signaling pathways involved in phosphate deficiency and the responses to auxin, cytokinin, and abscisic acid. Planta **227:** 1025–1036.

**Risseeuw, E.P., Daskalchuk, T.E., Banks, T.W., Liu, E., Cotelesage, J., Hellmann, H., Estelle, M., Somers, D.E., and Crosby, W.L.** (2003). Protein interaction analysis of SCF ubiquitin E3 ligase subunits from *Arabidopsis.* Plant J. **34:** 753–767.

**Robatzek, S., and Somssich, I.E.** (2001). A new member of the *Arabidopsis* WRKY transcription factor family, *At*WRKY6, is associated with both senescence- and defence-related processes. Plant J. **28:** 123–133.

**Rouached, H., Stefanovic, A., Secco, D., Bulak Arpat, A., Gout, E., Bligny, R., and Poirier, Y.** (2011). Uncoupling phosphate deficiency from its major effects on growth and transcriptome via PHO1 expression in Arabidopsis. Plant J. **65:** 557–570.

**Rubio, V., Linhares, F., Solano, R., Martín, A.C., Iglesias, J., Leyva, A., and Paz-Ares, J.** (2001). A conserved MYB transcription factor involved in phosphate starvation signaling both in vascular plants and in unicellular algae. Genes Dev. **15:** 2122–2133.

**Sadanandom, A., Bailey, M., Ewan, R., Lee, J., and Nelis, S.** (2012). The ubiquitin-proteasome system: central modifier of plant signalling. New Phytol. **196:** 13–28.

**Shin, H., Shin, H.S., Dewbre, G.R., and Harrison, M.J.** (2004). Phosphate transport in *Arabidopsis*: Pht1;1 and Pht1;4 play a major role in phosphate acquisition from both low- and high-phosphate environments. Plant J. **39:** 629–642.

**Smalle, J., and Vierstra, R.D.** (2004). The ubiquitin 26S proteasome proteolytic pathway. Annu. Rev. Plant Biol. **55:** 555–590.

**Stefanovic, A., Ribot, C., Rouached, H., Wang, Y., Chong, J., Belbahri, L., Delessert, S., and Poirier, Y.** (2007). Members of the *PHO1* gene family show limited functional redundancy in phosphate transfer to the shoot, and are regulated by phosphate deficiency via distinct pathways. Plant J. **50:** 982–994.

**Su, T., Xu, Q., Zhang, F.C., Chen, Y., Li, L.Q., Wu, W.H., and Chen, Y.F.** (2015). WRKY42 modulates phosphate homeostasis through regulating phosphate translocation and acquisition in Arabidopsis. Plant Physiol. **167:** 1579–1591.

**Tamura, K., Peterson, D., Peterson, N., Stecher, G., Nei, M., and Kumar, S.** (2011). MEGA5: molecular evolutionary genetics analysis using maximum likelihood, evolutionary distance, and maximum parsimony methods. Mol. Biol. Evol. **28:** 2731–2739.

**Waadt, R., and Kudla, J.** (2008). In planta visualization of protein interactions using bimolecular fluorescence complementation (BiFC). Cold Spring Harb. Protoc. **2008:** pdb.prot4995.

**Wang, Z., et al.** (2014). Rice SPX1 and SPX2 inhibit phosphate starvation responses through interacting with PHR2 in a phosphate-dependent manner. Proc. Natl. Acad. Sci. USA **111:** 14953–14958.